ISSN:2790-1688 DOI: 10.56028/aetr.4.1.230.2023

Analysis of spatial and temporal stress of waste concrete circular rock

Zhengbing Xia

College of Architecture and Civil Engineering, Jiangsu City Vocational College Nantong Campus, Nantong 226000, China

109779577@qq.com

Abstract. Different proportions of waste concrete are mixed into the surrounding rock with crushing agent, and the boundary moisture content, the linear shrinkage rate, the expansion force test, the compaction test, the unlimited compressive strength and the CBR test were verified under different curing times. The surrounding rock stress state has significant spatial-temporal effects. Around the stress evolution process of the surrounding rock in the roadway excavation, the space-time effect of the surrounding rock stress distribution of the circular roadway under the uniform stress field is preliminarily analyzed, and the correlation of time and space and other related parameters is discussed. The study shows that the XiYuan model can fully reflect the stress relaxation effect of surrounding rock, and the three-way stress decreases with time and finally stabilizes in a certain balance state. In the early stage, the more obvious the stress concentration, the stress relaxation; the mechanical relaxation behavior of surrounding rock is a space-time function, the radial stress decreases with the rear distance of the excavation surface, and the annular stress is just opposite, while the axial stress remains unchanged. This study can provide a theoretical basis for the stability prediction and evaluation of rock mass roadway engineering.

Keywords: circular roadway; earth stress; western yuan model; space-time effect; evolution.

1. surrounding rock stress, spatiotemporal evolution model

Figure 1 presents a spatiotemporal evolution model of the circular roadway surrounding rock stress under the uniform stress field. The basic assumptions of the model are:

(1) The section without supported tunnel is regarded as circular with ground stress p0For uniform stress; the mechanical behavior of the section far away from the excavation surface follows the plane strain assumption; the mechanical behavior of surrounding rock shows stress relaxation in time scale and follows the XiYuan model[7-8](As shown in Figure Figure 22);

(2) The severe deformation in the initial stage of tunnel excavation does not consider the viscous response of the surrounding rock, and the relatively stable deformation stage is relatively small because of the surrounding rock displacement, so the relaxation effect of the surrounding rock stress redistribution can be regarded as a mechanical problem under the condition of constant deformation[9];

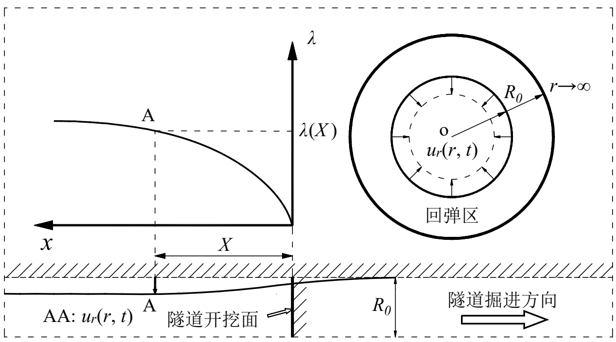

Figure 1. Spatiotemporal evolution model of surrounding rock stress in circular lane

Considering the spatial effect of the excavation surface, the imaginary support force at different sections of the tunnel[1][10]Not consistent with the amount of convergence, as shown in Figure1. In

ISSN:2790-1688 DOI: 10.56028/aetr.4.1.230.2023

view of this effect, Panet, Vlachopoulos and many other scholars have proposed the characteristic equations to describe the stress and displacement release rate of surrounding rock[1][11]; However, the Panet method overestimates the hole circumference displacement to make the design more than unsafe[1]; The Vlachopoulo s method must first obtain the maximum plastic zone radius of the surrounding rock[11], Is not suitable for the analysis of the viscoelastic problems. After careful consideration, the selection of E. Hoek, the fitting equation given[1]To calculate:

$$\lambda(X)=\left[1+\exp\left(\frac{-X/R_0}{1.10}\right)\right]^{-1.7} \quad (1)$$

2. Organization of the Text Circular lane surrounding rock stress, space-time evolution, theoretical calculation

As shown in Figure 2, the Westyuan model is composed of viscoplastic body and generalized K elvin body; when the one-dimensional stress is less than the long-term strength of surrounding rock σsWhen, the Westyuan model degenerated to a generalized K elvin model.

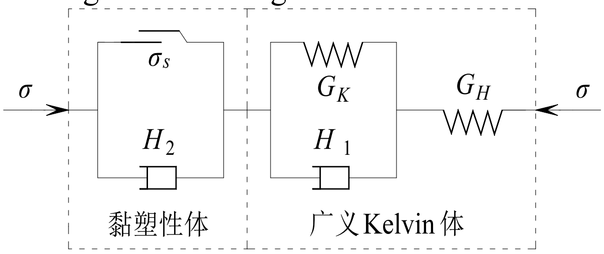

Figure 2 ishihara model

$$S_{ij}(t)=2G_1(t)\left(e_{ij}\right)_0 \quad (2)$$

$$S_{ij}(t)=2G_2(t)\left(e_{ij}\right)_0+\frac{\sigma_s}{p_2}\left[p_2+\frac{p_2}{\sqrt{p_1^2-4p_2}}\cdot\left(\frac{\exp(-\alpha t)}{\alpha}-\frac{\exp(-\beta t)}{\beta}\right)\right] \quad (3)$$

Where, Sij、eijRepresents the partial stress tensor and partial strain tensor of surrounding rock under 3 D stress state respectively; GH、GKAnd H1、H2The shear modulus (MPa) and viscous coefficient (MPa · h) of the Westhara model, respectively.

According to the elastic mechanics, the partial stress tensor SijWith the partial-strain tensor eijThe following relationships exist:

$$\left.\begin{aligned}S_{ij}&=\sigma_{ij}-\delta_{ij}\sigma_m\\ \sigma_m&=\frac{1}{3}\left(\sigma_\theta+\sigma_z+\sigma_r\right)\end{aligned}\right\} \quad (4)$$

$$\left.\begin{aligned}e_{ij}&=\varepsilon_{ij}-\delta_{ij}\varepsilon_m\\ \varepsilon_m&=\frac{1}{3}\left(\varepsilon_\theta+\varepsilon_z+\varepsilon_r\right)\end{aligned}\right\} \quad (5)$$

This study only addressed the elastic force response of surrounding rock, so σ <σ was used in the Westhara modelscircumstances. Add equation (4) and (5) to the relaxation equation (2)

$$2G_1(t)\left[2\left(\varepsilon_\theta\right)_0-\left(\varepsilon_r\right)_0-\left(\varepsilon_z\right)_0\right] \quad (6)$$

Based on the plane strain assumption, there is[12]

ISSN:2790-1688 DOI: 10.56028/aetr.4.1.230.2023

$$\begin{cases}\sigma_z(t)=\mu\left[\sigma_\theta(t)+\sigma_r(t)\right] \\ (\varepsilon_z)_0=0\end{cases} \quad (7)$$

Where the μ is the Poisson's ratio.Joint vertical formula (6), (7), then

$$2G_1(t)\left[2(\varepsilon_\theta)_0-(\varepsilon_r)_0\right] \quad (8)$$

$$2G_1(t)\left[2(\varepsilon_r)_0-(\varepsilon_\theta)_0\right] \quad (9)$$

Joint vertical formula (8), (9), yes

$$\begin{cases}(1-\mu)\sigma_\theta(t)-\mu\sigma_r(t)=2G_1(t)(\varepsilon_\theta)_0 \\ (1-\mu)\sigma_r(t)-\mu\sigma_\theta(t)=2G_1(t)(\varepsilon_r)_0\end{cases} \quad (10)$$

equilibrium equation:

$$\frac{d\sigma_r(r,t)}{dr}=\frac{\sigma_\theta(r,t)-\sigma_r(r,t)}{r} \quad (11)$$

Joint vertical formula (10) and (11), then

$$\begin{aligned}(\varepsilon_\theta)_0&=\frac{(1-\mu)}{2G_1(t)}\frac{d\left[r\sigma_r(t)\right]}{dr}-\frac{\mu}{2G_1(t)}\sigma_r(t) \\ &=\frac{1-2\mu}{2G_1(t)}\sigma_r(t)+\frac{(1-\mu)}{2G_1(t)}r\frac{d\sigma_r(t)}{dr}\end{aligned} \quad (12)$$

$$(\varepsilon_r)_0=\frac{(1-\mu)}{2G_1(t)}\sigma_r(t)-\frac{\mu}{2G_1(t)}\frac{d\left[r\sigma_r(t)\right]}{dr} \quad (13)$$

The force deformation of the surrounding rock under the uniform stress field shall meet the strain coordination equation, as follows:

$$\frac{d(\varepsilon_\theta)_0}{dr}=\frac{(\varepsilon_r)_0-(\varepsilon_\theta)_0}{r} \quad (14)$$

Is available by Equation (14)

$$(\varepsilon_r)_0=\frac{d\left[r(\varepsilon_\theta)_0\right]}{dr} \quad (15)$$

Put formula (12) into (15)

$$\begin{aligned}(\varepsilon_r)_0=&\frac{1-2\mu}{2G_1(t)}\left[\sigma_r(t)+r\frac{d\sigma_r(t)}{dr}\right]+ \\ &\frac{(1-\mu)}{2G_1(t)}\left[2r\frac{d\sigma_r(t)}{dr}+r^2\frac{d^2\sigma_r(t)}{dr^2}\right]\end{aligned} \quad (16)$$

Joint vertical type (13) and (16), collated and obtained

$$r\frac{d^2\sigma_r(r,t)}{dr^2}+3\frac{d\sigma_r(r,t)}{dr}=0 \quad (17)$$

set up c1、c2For the integral constant, the radial stress expression can be obtained from Equation (17):

$$\sigma_r(r,t)=-\frac{c_1}{2r^2}+c_2 \quad (18)$$

Joint equilibrium equation (11), can get the circumferential stress expression:

ISSN:2790-1688 DOI: 10.56028/aetr.4.1.230.2023

$$\sigma_\theta(r,t)=\frac{c_1}{2r^2}+c_2 \quad (19)$$

Put formula (18) and (19) into (12)

$$\begin{cases} c_1 = 2G_1(t)\left[(\varepsilon_\theta)_0-(\varepsilon_r)_0\right]r^2 \\ c_2 = \dfrac{2G_1(t)\left[(\varepsilon_\theta)_0+(\varepsilon_r)_0\right]}{2(1-2\mu)} \end{cases} \quad (20)$$

The severe deformation in the initial stage of tunnel excavation, so the circumferential strain of stress release rate is considered as follows:

$$(\varepsilon_\theta)_0=\frac{(1+\mu)p_0}{E}\left[(1-2\mu)+\lambda(X)\left(\frac{R_0}{r}\right)^2\right] \quad (21)$$

Joint strain coordination equation (14) provides radial strain

$$(\varepsilon_r)_0=\frac{(1+\mu)p_0}{E}\left[(1-2\mu)-\lambda(X)\left(\frac{R_0}{r}\right)^2\right] \quad (22)$$

Add ate (21) and (22) into (20)

When t =0, the present solution and Fahimifar solution[12], G oodman solution[14]Consistently, the correctness of stress, spatial and space evolution, theoretical calculation. The theoretical calculation can reflect both the relaxation effect of surrounding rock stress and the influence of excavation surface, which is superior compared with the solution in literature [2-5].

3. Analysis of the spatial and temporal evolution of the surrounding rock stress in the circular lane

In the discussion analysis, according to ref[8]Westhara model parameters were selected as shown in Table 1. Also, refer to the example[12]：R0=4.57m，p0=6.897MPa，μ=0.2。

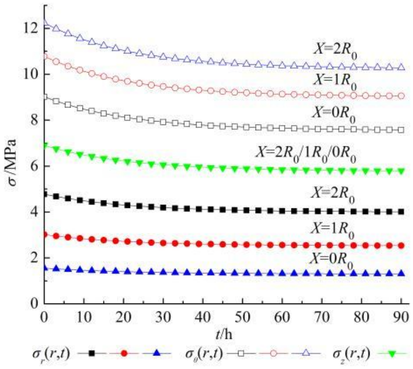

Figure 3 Three-way stress of hole walls in different sections

Figure 3 shows the different sections (X =0R0，1R0，2R0) The spatiotemporal evolution curve of annular, axial and radial stress of surrounding rock. It can be seen from the figure that the western Yuan model can fully reflect the relaxation effect of surrounding rock stress, and the three-way stress decreases with time and finally stabilizes in a certain equilibrium state. In the early stage of stress relaxation, the decrease speed of the first main stress is significantly greater than the second and third main stress, and the more obvious the stress concentration, the more significant the stress relaxation. In addition, compared with the section of the near excavation surface, the three-way stress relaxation speed of the distant section is quite different, which shows the radial

ISSN:2790-1688 DOI: 10.56028/aetr.4.1.230.2023
decrease, the ring direction increase while the axial direction does not change. It can be seen that the influence of the circumferential and radial stress relaxation behavior facing the excavation wall is different. Figures 4 and 5 can also reflect this rule.

Figures 4 and 5 show the distribution curves of the radial and circumferential stresses in the longitudinal direction of the tunnel. As shown from Figure 4, the closer to the excavation surface, the greater the radial stress, the greater the relaxation speed; the distant section is almost not affected by the excavation surface. At the beginning of the hole, the stress relaxation effect is obvious, and the stress gradually stabilizes over time. As can be seen from Figure 5, the farther away from the excavation surface, the greater the annular stress, but the evolution rate is close to zero. Compared with the early stage of the hole, the stress relaxation effect in the later stage is not obvious. It can be seen that the relaxation effect of surrounding rock stress is a function of space and time. In time, the longer the duration, the less obvious the relaxation effect; In space, the farther from the excavation surface, the less obvious the relaxation effect, which is consistent with literature [3].

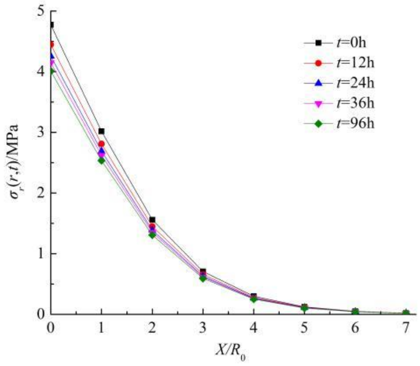

Figure 4 Longitudinal distribution curve of the radial stress of the hole wall

Fig.4 Axial distribution curve of the radial stress at tunnel wall

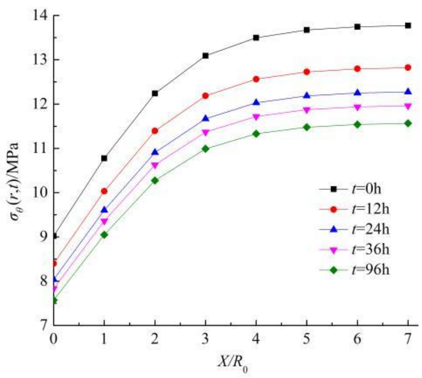

Figure 5. Longitudinal distribution curve of the annular stress of the hole wall

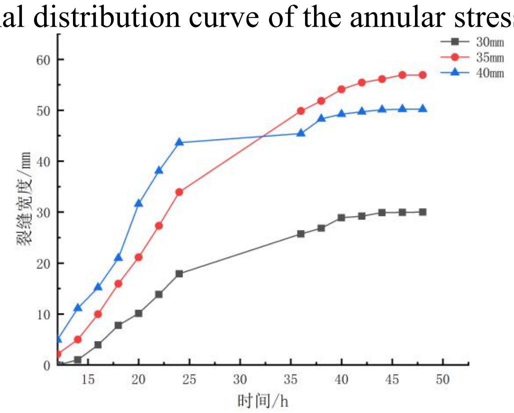

ISSN:2790-1688 DOI: 10.56028/aetr.4.1.230.2023

Figure 6 Breaking time- -crack width relationship curve of concrete blocks with different pore sizes

4. Breaking effect and analysis of concrete blocks of different drilling holes

Representative pictures of loading and crushing effect of cloblocks during static crushing are shown in Figure 7 and Figure 8, respectively. In order to describe the phenomenon, the crack width used in describing and analyzing the test phenomenon is the surface width. In order to compare the crushing effect of different boreholes, with the crushing time of concrete block as the horizontal axis and the development width of cracks as the vertical axis, the relationship curve is shown in Figure 9.

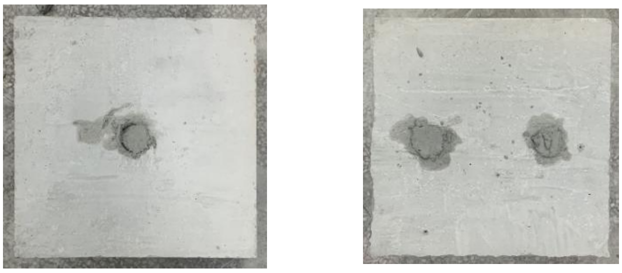

(A) Single hole of 35 mm (B) Double hole of 35 mm

Figure 7 After charging of concrete test blocks with different drilling numbers

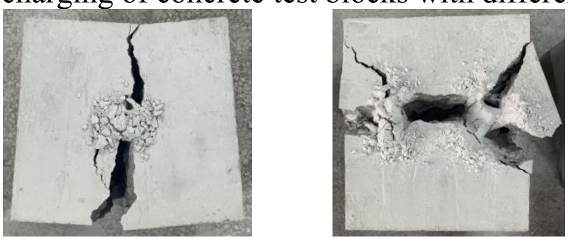

(A) Single hole of 35 mm (D) Double hole of 35 mm

Figure 8 After the concrete test blocks of different number of boreholes are broken

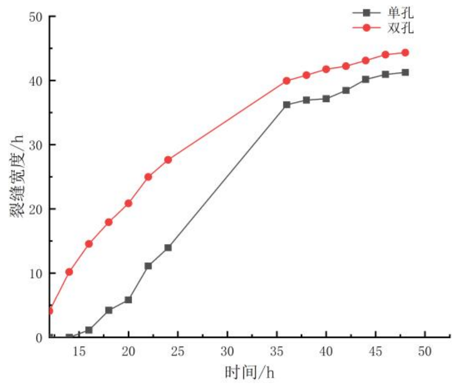

Figure 9 Breaking time-relationship curve of crack width of concrete blocks with different drilling holes

According to the test combined with Figure 7 and 8, and comparing the test phenomenon of different bored concrete blocks in the static crushing process, it is found that:

(1) After 48 h of crushing, the cracks of the single hole 35 mm and double hole 35mm concrete test block are basically "one" type, but the double hole 35 mm concrete test block has derived some small cracks around the main cracks. The single hole 35 mm and double hole 35 mm concrete test block are no. 14.95 h and 10.45 h respectively, and the time of the first crack increase from single hole 35 mm to double hole 35 mm advances by 4.5 h. When other conditions are the same, the time

ISSN:2790-1688 DOI: 10.56028/aetr.4.1.230.2023

of the increase of the number of holes, the reason may be that the larger the number of holes, the larger the charge, the expansion pressure increases, which will accelerate the formation of the crack and advance the time of the first crack.

(2) The crack width of the single-hole 35 mm concrete test block after 48 h is 41.26 mm, From loading completion to 48 h of cracking, Aan hourly crack width increase of about 0.86 mm, The crack width of the double-hole 35 mm concrete test block is 44.34 mm, From loading completion to 48 h of cracking, Aan hourly crack width increase of about 0.92 mm, And whether it is a single 35 mm concrete block or a double 35 mm concrete block, The crack development rate is basically increased first and then reduced, It can be found that when all other conditions are the same, As the number of boreholes was increased, The average hourly crack width of the concrete test block will increase slightly, It indicates that the more drilled holes, the better the crushing effect. In addition, from the perspective of the crack generation time and width, the crack width produced by the double hole 35 mm concrete test block at any recorded time point is greater than the crack width produced by the single hole 35 mm concrete test block, and the difference is basically increased first and then reduced, which shows that the crushing effect of the double hole 35 mm concrete test block is better than that of the single hole 35 mm concrete test block.

The hit curves fitted by the experimental results are shown in Figure 10. When adding 12% abandoned concrete blocks, the maximum dry density ranges from 1.77g / cm3Increase to 1.81g / cm3, The optimal moisture content decreased from 17.5% to 16.3%. The decrease of the optimal moisture content is the existence of fine sand in the abandoned concrete blocks, which is hard and is not easy to absorb too much water. Compared with clay, its internal space is loose and its specific surface area is usually low. This conclusion is consistent with Yang Jun's research in the improvement of expanded soil by natural gravel.

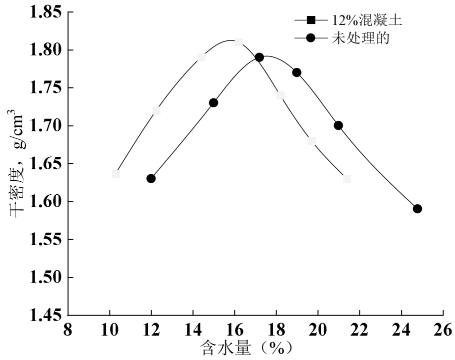

Fig.10. Curve of moisture content and dry densitySummary

5. The Conclusion

In this paper, the space-time evolution model of the surrounding rock under the uniform stress field, and calculates the stress distribution problem under the spatial effect of the excavation surface. Finally, the correlation of time, space and parameters, and the following conclusions:

(1) The Xiyuan model can fully reflect the relaxation effect of surrounding rock stress, and the three-way stress decreases with time to stabilize in a certain equilibrium state.

(2) In the initial stage of stress relaxation, the decay rate of the first main stress is significantly greater than the second and third main stresses, and the more obvious the stress concentration, the more significant the stress relaxation.

(3) Compared with the section of the near excavation surface, the three-way stress relaxation speed of the distant section is quite different, which shows that the annular direction increases, the radial direction decreases and the axial direction remains unchanged.

(4) The mechanical relaxation behavior of surrounding rock is a function of space and time. The farther away from the excavation surface or the longer the duration is, the less obvious the relaxation effect is.

ISSN:2790-1688 DOI: 10.56028/aetr.4.1.230.2023

(5) Because the concrete waste material is a non-viscous material, the liquid limit, plasticity index and linear shrinkage limit of the treated soil decrease with the increase of the percentage of soil mixed concrete, and the plastic limit is slightly increased.

The above conclusion has certain reference value for the stability prediction of rock mass roadway engineering, and the calculation idea still needs to be further improved combined with the actual situation.

References

[1] Sun Jun. Several advances in rock rheology and its engineering applications [J]. Journal of Rock mechanics and Engineering, 2007,26 (6): 1081-1106.

[2] Paraschiv-Munteanu I, Cristescu N .D.Stress Relaxation during Creep of Rocks around Deep Boreholes [J].International Journal of Engineering Science, 2001, 39(7): 737-754.

[3] King Chao, Chen Weizhong, Qiao Liping, Zhang Lewen. Preliminary theoretical solution to the stress relaxation effect in underground engineering [J]. Journal of Rock Mechanics and Engineering, 2010,29 (A02): 4096-4101.

[4] Fan Pengxian, Wang Mingyang, Li Wenpei, Chen Mingxiong. Time effect of surrounding rock stress deformation during the unloading process of deep buried tunnel [J]. Rock and Soil Mechanics, 2010,31 (S1): 28-34.

[5] Wang Xiangyu, Bai Jianbiao, Chen Yong, Hu Zhongchao. Stress relaxation effect and control technology in deep well roadway [J]. Journal of Coal Science, 2010,35 (7): 1072-1077.

[6] Liu Ning, Zhang Chunsheng, Chen Xiangrong, Hou Jing, Chu Weijiang. Monitoring and characteristics of surrounding rock in deep buried tunnel [J]. Journal of Rock mechanics and Engineering, 2011,30 (9): 1729-1737.

[7] Tian Hongming, Chen Weizhong, Zhao Wusheng, Tian Tian, Yuan Kekuo. Study on the stress relaxation characteristics of muddy red sandstone on Yi-Ba Expressway [J]. Rock and soil mechanics, 2013,34 (4): 981-986.

[8] Tian Hongming, Chen Weizhong, Xiao Zhenglong, Wu Guojun, Han Guangqin. Experimental study on high circumference pressure of muddy siltstone [J]. Journal of Geotechnical Engineering, 2015,37 (8): 1433-1439.

[9] Yu Huaichang, Li Yali, Liu Handong. Study on constitutive model of compressive stress relaxation in silty mudstone [J]. Coal Journal, 2011,36 (8): 1258-1263.

[10] Hou Gongyu, Niu Xiaosong. An ideal elastic-plastic solution of an axisymmetric circular lane based on the Levy-Mises constitutive relation and the Hoek-Brown yield criterion [J]. Journal of Rock mechanics and Engineering, 2010,29 (4): 765-777.

[11] Vlachopoulos N, Diederichs M .S .Improved L ongitudinal D isplacements P rofiles for C onvergence C onfinement A nalysis of D eep T unnel.Rock Mechanics and Rock Engineering , 2009, 42: 131-146.

[12] Fahimifar A, Tehrani F .M, Hedayat A, Vakilzadeh A.Analytical S olution for the E xcavation of C ircular T unnels in a V isco-elastic Burger's M aterial under H ydrostatic S tress F ield [J].Tunnelling and Underground Space Technology, 2010, 25(4): 297-304.

[13] Brady B .H .G, Brown E .T.Rock M echanics: for U nderground M ining [M].Springer Science & Business Media, 2013.

[14] Goodman, R.E.(1989) Introduction in Rock Mechanics.2ndedn.John Wiley & Sons Ltd, New York.